RELEASE DATE
MAR 11 1957

NACA RM H57A16

Copy
RM H57A16

1

PERMANENT FILE COPY

CONFIDENTIAL

# NACA

# RESEARCH MEMORANDUM

FLIGHT-DETERMINED STATIC LATERAL STABILITY AND CONTROL

CHARACTERISTICS OF A SWEPT-WING FIGHTER

AIRPLANE TO A MACH NUMBER OF 1.39

By Gene J. Matranga and James R. Peele

High-Speed Flight Station
Edwards, Calif.

# NATIONAL ADVISORY COMMITTEE
# FOR AERONAUTICS
## WASHINGTON
March 11, 1957

CONFIDENTIAL

CLASSIFICATION CANCELLED

CONFIDENTIAL

NATIONAL ADVISORY COMMITTEE FOR AERONAUTICS

RESEARCH MEMORANDUM

FLIGHT-DETERMINED STATIC LATERAL STABILITY AND CONTROL

CHARACTERISTICS OF A SWEPT-WING FIGHTER

AIRPLANE TO A MACH NUMBER OF 1.39

By Gene J. Matranga and James R. Peele

SUMMARY

The static lateral stability characteristics of a swept-wing fighter-type airplane incorporating three vertical-tail configurations and two wing configurations were investigated at an altitude of 40,000 feet over a Mach number range from 0.72 to 1.39. The data obtained were determined during constant-heading sideslips and wings-level turns, aileron rolls, and abrupt rudder pulses.

The apparent dihedral parameter $\frac{d\delta_{a_t}}{d\beta}$, the apparent aileron effectiveness parameter $\frac{pb}{2V}\Big/\delta_{a_t}$, the aileron effectiveness derivative $C_{l_{\delta_{a_t}}}$, the rudder effectiveness derivative $C_{n_{\delta_r}}$, and the rolling moment due to rudder deflection $C_{l_{\delta_r}}$ remained essentially constant up to high transonic speeds. With a further increase in Mach number the values of these derivatives decreased.

The apparent directional stability parameter $\frac{d\delta_r}{d\beta}$ remained nearly constant below the transonic region but increased in value with a further increase in Mach number.

The trimmed lateral-force derivative $C_{Y_\beta}$ and the yawing moment due to aileron deflection $C_{n_{\delta_{a_t}}}$ exhibited little change through the speed range tested.

With an increase in vertical-tail size and wing span a noticeable difference in the values of $\frac{d\delta_r}{d\beta}$, and a slight difference in the values of $C_{l_{\delta_{a_t}}}$ and $C_{n_{\delta_r}}$ were evident for any given Mach number.

CONFIDENTIAL

## INTRODUCTION

A universal interest has been exhibited in handling-qualities flight data in the transonic and supersonic regions because of the large changes in stability and control characteristics in this area.  In order to furnish a better understanding of these phenomena for current and future aircraft designs, a 45° swept-wing fighter-type airplane was procured by the U. S. Air Force for flight testing by the NACA High-Speed Flight Station at Edwards, Calif.

Several flight investigations with the subject airplane in the transonic and supersonic region have been performed and reported (refs. 1 to 4).  These investigations, as well as the present one, employed three different vertical tails with varying aspect ratio or area, or both, and two wing configurations - the basic wing, and the basic wing plus wing-tip extensions.

This paper presents the overall static lateral stability and control characteristics generally for a pressure altitude of 40,000 feet and a Mach number range from 0.72 to 1.39.

## SYMBOLS

All coefficients and moments of inertia are referenced to the body axes and are based on the geometric dimensions of the particular configuration under consideration.

$A$          aspect ratio, $\dfrac{b^2}{S}$

$a_n$         normal acceleration, g units

$a_t$         transverse acceleration, g units

$b$          wing span, ft

$C_l$         rolling-moment coefficient, $\dfrac{L}{qSb}$

$C_{l_{\delta_{a_t}}}$       aileron effectiveness derivative, $\dfrac{dC_l}{d\delta_{a_t}}$, per deg

$C_{l_{\delta_r}}$       $\dfrac{dC_l}{d\delta_r}$, per deg

$C_{N_A}$        airplane normal-force coefficient, $\dfrac{W a_n}{qS}$

$C_n$        yawing-moment coefficient, $\dfrac{N}{qSb}$

$C_{n_{\delta_{a_t}}}$        $\dfrac{dC_n}{d\delta_{a_t}}$, per deg

$C_{n_{\delta_r}}$        rudder effectiveness derivative, $\dfrac{dC_n}{d\delta_r}$, per deg

$C_Y$        airplane lateral-force coefficient, $\dfrac{W a_t}{qS}$

$C_{Y_\beta}$        lateral-force derivative, $\dfrac{dC_Y}{d\beta}$, per deg

$c$        chord, ft

$\dfrac{d\delta_{a_t}}{d\beta}$        apparent dihedral parameter

$\dfrac{d\delta_r}{d\beta}$        apparent directional stability parameter

$g$        acceleration due to gravity, ft/sec$^2$

$h_p$        pressure altitude, ft

$I_X$        moment of inertia about X-axis, slug-ft$^2$

$I_Y$        moment of inertia about Y-axis, slug-ft$^2$

$I_Z$        moment of inertia about Z-axis, slug-ft$^2$

$I_{XZ}$        product of inertia, $1/2\left(I_Z - I_X\right)\sin \epsilon$, slug-ft$^2$

$i_t$        angle of tail incidence measured from line parallel to X-axis of airplane, positive when leading edge deflected up, deg

$L$        rolling moment, ft-lb

$M$        Mach number

N         yawing moment, ft-lb

p         rolling angular velocity, radians/sec

$\dot{p}$         rolling angular acceleration, radians/sec$^2$

$\frac{pb}{2V}\Big/\delta_{a_t}$         apparent aileron effectiveness parameter

q         dynamic pressure, $\frac{1}{2}\rho V^2$, lb/sq ft

r         yawing angular velocity, radians/sec

$\dot{r}$         yawing angular acceleration, radians/sec$^2$

S         wing area, sq ft

V         true velocity, ft/sec

W         airplane weight, lb

$\alpha$         angle of attack, deg

$\beta$         angle of sideslip, deg

$\delta_{a_t}$         total aileron deflection, positive for right roll, deg

$\delta_r$         rudder deflection, positive when deflected left, deg

$\epsilon$         angle between body X-axis and principal X-axis, positive when body axis is above principal axis at airplane nose, deg

$\Lambda_c/4$         sweepback angle at the quarter chord, deg

$\lambda$         taper ratio

$\rho$         mass density of air, slugs/cu ft

## AIRPLANE

The airplane used in this investigation is a fighter type with low, swept wings, and incorporates midsemispan ailerons and a low, swept horizontal tail. On the leading edge of the wings there were free-floating slats which were normally closed during all phases of this investigation.

A single turbojet engine with afterburner powers the airplane.  The
investigation covered the following four configurations which involved
three different vertical tails and two different wing configurations:

| Configuration | Vertical tail | | | Wing | | |
|---|---|---|---|---|---|---|
| | Tail designation | Area, sq ft | Aspect ratio | Area, sq ft | Span, ft | Aspect ratio |
| A | A | 33.5 | 1.13 | 376 | 36.6 | 3.56 |
| B | B | 37.3 | 1.49 | 376 | 36.6 | 3.56 |
| C | C | 42.7 | 1.49 | 376 | 36.6 | 3.56 |
| D | C | 42.7 | 1.49 | 385 | 38.6 | 3.88 |

A three-view drawing and a photograph of the airplane, with the
configuration incorporating the largest vertical tail and the increased
wing span, are shown in figures 1 and 2, respectively.

A photograph showing vertical tails A and C and drawings of the
three tails defining the areas are shown in figures 3 and 4, respectively.
In all configurations the same rudder was used.

The physical characteristics of the original airplane (configura-
tion A) and the modifications tested are presented in table I.  Figure 5
shows the variation of the moments of inertia about the body axes and
the principal axis inclination relative to the body axis based on the
manufacturer's estimates for weight conditions expected in the normal
flight range.

## INSTRUMENTATION

The following quantities pertinent to this investigation were
recorded on NACA internal recording instruments synchronized by a com-
mon timer:

        Airspeed and altitude
        Normal and transverse acceleration
        Angle of attack and angle of sideslip
        Aileron, rudder, and stabilizer deflections
        Rolling, pitching, and yawing velocities and accelerations

The angle of attack, angle of sideslip, airspeed, and altitude
were sensed on the nose boom.  The angle of attack and angle of side-
slip were corrected for pitching and yawing velocities, respectively.

The airspeed system was calibrated by the NACA radar phototheodolite method and is considered accurate to $M = \pm 0.02$ at subsonic speeds and $M = \pm 0.01$ at supersonic speeds. (Additional discussion of the accuracies may be found in reference 2.) The turn meters used to measure the angular velocities and accelerations were referenced to the body axes of the airplane. The weight of the airplane was obtained from the pilot's report of the fuel remaining before each maneuver.

## TESTS

The tests for all four airplane configurations were conducted in the clean configuration with the center-of-gravity position at about 32 percent of the mean aerodynamic chord of the original wing; however, for configuration D the center-of-gravity position based on the mean aerodynamic chord of the extended wing was at about 30 percent. The data were obtained within the Mach number range from 0.72 to 1.39 at a pressure altitude of 40,000 feet with the exception of limited data obtained near a Mach number of 0.75 and 30,000 feet and a Mach number of 0.40 and 15,000 feet.

The characteristics in sideslip were obtained from constant-heading sideslip maneuvers and, in addition, wings-level turns for configuration D only. The lateral control effectiveness was determined during abrupt rudder-fixed aileron rolls at various control deflections up to full aileron deflection, except for configurations A and B which were limited to approximately one-third and two-thirds total aileron deflection, respectively. Limiting the aileron deflection was necessary because of the violent lateral-longitudinal coupling and roll behavior encountered with configurations A and B (refs. 3 and 4). A chain stop on the control stick was used to obtain constant aileron input. This investigation also includes data from abrupt rudder pulses to obtain control effectiveness derivatives.

All maneuvers used in this investigation were performed at or initiated from 1 g level-flight conditions. Nominal angle-of-attack and normal-force-coefficient variations with Mach number are presented in figure 6 for the 1 g level-flight condition of this investigation.

It should be noted that all derivatives used in this paper are based on the physical dimensions of the particular configuration under consideration.

## RESULTS AND DISCUSSION

### Sideslip Characteristics

Representative plots of the variation of aileron, rudder, and stabilizer positions, and transverse acceleration with angle of sideslip at a Mach number of 0.73 and an altitude of 30,000 feet and at Mach numbers of 1.0 and 1.15 at 40,000 feet are presented in figure 7. Data for all four airplane configurations are included, except at a Mach number of 1.15 (fig. 7(c)). At this Mach number there are no data for configuration C since the investigation with this configuration did not extend beyond a Mach number of 1.0. The variations of rudder and aileron deflections and transverse acceleration with sideslip angle generally were linear over the ranges tested. There was evidence of only slight pitching-moment changes with sideslip, as shown by the variation of stabilizer position with sideslip angle.

The variations of the apparent dihedral parameter $\frac{d\delta_{a_t}}{d\beta}$, the apparent directional stability parameter $\frac{d\delta_r}{d\beta}$, and the lateral-force derivative $C_{Y_\beta}$ as determined from sideslip maneuvers over the Mach number range covered are summarized for the four configurations in figure 8. The apparent dihedral parameter $\frac{d\delta_{a_t}}{d\beta}$ shows little or no change among the different configurations and is positive except at Mach numbers above $M \approx 1.34$, as shown for configurations B and D. Although the apparent dihedral parameter $\frac{d\delta_{a_t}}{d\beta}$ remains fairly constant at values near one below a Mach number of about 0.92, it decreases abruptly to nearly zero in the Mach number range between 1.0 and 1.05. Above this range there is a slight increase in the apparent dihedral to a value approximately one-half the subsonic value. The data for configurations B and D in figure 8 at a Mach number of 0.73 show that the apparent dihedral parameter $\frac{d\delta_{a_t}}{d\beta}$ is decreased with a decrease in altitude. This decrease in $\frac{d\delta_{a_t}}{d\beta}$ noted between the two altitudes is primarily the result of a decrease of 3° in angle of attack (fig. 6). A comparison of the low-speed value of $\frac{d\delta_{a_t}}{d\beta}$ at an altitude of 15,000 feet with the value at a Mach number of 0.75 and an altitude of 40,000 feet (at comparable angles of attack) shows agreement.

The apparent directional stability parameter $\frac{d\delta_r}{d\beta}$ for the four
configurations is positive and below a Mach number of approximately 0.90
remains essentially constant, with values ranging from 1.6 for configu-
ration A to 2.6 for configuration D. Above this Mach number there is
an increase of $\frac{d\delta_r}{d\beta}$ to a value at supersonic speeds of more than 2 times
the subsonic value for configuration A and more than $2\frac{1}{2}$ times the subsonic
value for configuration D. The low-speed, low-altitude value of $\frac{d\delta_r}{d\beta}$
for configuration D is about the same as the value obtained at higher
altitude at a Mach number of 0.75. With increase in vertical-tail size
there is generally an increase in the value of $\frac{d\delta_r}{d\beta}$. Since the different
vertical tails all have the same rudder, the increase in apparent direc-
tional stability for any given Mach number with increased vertical-tail
size points to an increase in directional stability (ref. 1) instead of
a loss in rudder effectiveness. However, for any one configuration the
increase in $\frac{d\delta_r}{d\beta}$ with Mach number above the transonic region results
mainly from the loss in rudder effectiveness, as will be seen in a sub-
sequent section.

The trimmed lateral-force derivative $C_{Y_\beta}$ shows little or no change
among the configurations or with increase in Mach number except for a
slight increase near a Mach number of 1.0 for configuration A and above
a Mach number of 1.15 for configuration D, all values being approxi-
mately -0.008. The value for the low-speed, low-altitude test point
for configuration D is slightly higher than the other values at higher
altitudes.

For configuration D, wings-level turns were investigated and the
data were incorporated with the constant-heading sideslip data in fig-
ure 8(b). There was no difference noted in the parameters obtained in
this manner, although in the speed range where the dihedral was lowest,
there seemed to be less scatter in the aileron-position data.

## Lateral Control

The apparent aileron effectiveness parameter $\frac{pb}{2V}\Big/\delta_{a_t}$ obtained from
abrupt rudder-fixed aileron rolls was essentially linear throughout the
entire control and Mach number range investigated. Figure 9 shows typi-
cal variations of the helix angle with aileron deflection for Mach num-
bers of 0.73 and 1.25 at altitudes of 30,000 and 40,000 feet, respectively.

Figure 10 summarizes the Mach number variation of the apparent aileron effectiveness parameter $\frac{pb}{2V}\big/\delta_{a_t}$ for the four configurations.

The apparent aileron effectiveness parameter $\frac{pb}{2V}\big/\delta_{a_t}$ for configurations B and D remains nearly constant at a value of 0.0026 to a Mach number of about 0.90. Above a Mach number of 0.90 there is a gradual decrease in effectiveness to about 70 percent of the subsonic value near a Mach number of 1.3. Although there is little data for configurations A and C, the data show no appreciable change from the data obtained for configuration B. This is to be expected since the only difference in these three configurations is the size of the vertical tails, and the difference in the damping-in-roll contributed by the vertical tails would be negligible. The increase of 2 feet in wing span of configuration D does not appear to change the apparent aileron effectiveness below a Mach number of about 1.0; however, above $M = 1.0$ there is a slight decrease in apparent aileron effectiveness compared with the other configurations. This decrease results primarily from a loss in aileron effectiveness, as will be discussed in a following section. The low-speed, low-altitude data for configuration D again are similar to the other subsonic data in magnitude, although there is no reason to expect such similarity, considering compressibility effects, aeroelasticity, and possible change in roll damping.

### Control Effectiveness Derivatives

By using the methods discussed in the appendix and reference 5, the control effectiveness derivatives $C_{l_{\delta_{a_t}}}$, $C_{n_{\delta_{a_t}}}$, $C_{n_{\delta_r}}$, and $C_{l_{\delta_r}}$ were obtained for configurations B and D. Figure 11 presents the variation of these control effectiveness derivatives with Mach number.

In both configurations the aileron effectiveness derivative $C_{l_{\delta_{a_t}}}$ decreases fairly rapidly from relatively constant values of about 0.0010 for configuration B and about 0.0009 for configuration D below a Mach number of about 0.90 to less than one-half these values at a Mach number of 1.25. The low-speed, low-altitude data for configuration D are slightly higher in magnitude than the values of the transonic data at an altitude of 40,000 feet. The values of $C_{l_{\delta_{a_t}}}$ for configuration D are consistently smaller than the values for configuration B. This difference is accounted for at subsonic speeds by considering the difference in physical dimensions of the particular configuration employed in determining the derivatives. However, at supersonic speeds there is a definite loss in aileron effectiveness with the increase in wing area.

Values of the rudder effectiveness derivative $C_{n_{\delta_r}}$ in the transonic region are about -0.0006 for configuration B and vary with Mach number in a manner similar to the aileron effectiveness derivative $C_{l_{\delta_{at}}}$, although $C_{n_{\delta_r}}$ seems to retain its subsonic effectiveness to a slightly higher Mach number. At subsonic speeds the values of $C_{n_{\delta_r}}$ are slightly smaller for configuration D than for configuration B. However, for supersonic speeds they are essentially the same for any given Mach number. A comparison of the low-speed, low-altitude values of $C_{n_{\delta_r}}$ for configuration D with data in the transonic region shows the data to be at almost the same level.

Very little change is exhibited in the variation with Mach number of the yawing moment due to aileron deflection $C_{n_{\delta_{at}}}$ which remained essentially constant at a value near 0.0002. The rolling moment due to rudder deflection $C_{l_{\delta_r}}$ remained constant at a value of about 0.0001 below a Mach number of 1.0; however, at the higher supersonic Mach numbers $C_{l_{\delta_r}}$ became zero. No measurable effect of airplane configuration on these parameters was apparent. For configuration D, one low-speed and low-altitude data point of $C_{n_{\delta_{at}}}$ and $C_{l_{\delta_r}}$ was of the same order of magnitude as the data obtained at higher speeds.

## CONCLUSIONS

From a static lateral flight investigation of three vertical-tail configurations and two wing configurations of a swept-wing fighter-type airplane, generally at an altitude of 40,000 feet and over a Mach number range from 0.72 to 1.39, it may be concluded that:

1. The apparent dihedral parameter $\dfrac{d\delta_{at}}{d\beta}$ shows little or no change among configurations. The value of $\dfrac{d\delta_{at}}{d\beta}$ is fairly constant at about 1.0 below a Mach number of 0.92, decreases to almost zero near a Mach number of 1.0, then regains about one-half its subsonic value at a Mach number of 1.20. Above a Mach number of 1.34 the value becomes slightly negative.

2. The apparent directional stability parameter $\dfrac{d\delta_r}{d\beta}$ shows an increase in value with increase in vertical-tail size. The derivative

$\frac{d\delta_r}{d\beta}$ remains generally constant below a Mach number of about 0.90, with values ranging from 1.6 to 2.6, depending on the configuration. Above this Mach number there is an increase to a value at supersonic speeds of about 2 to $2\frac{1}{2}$ times the subsonic values.

3. The lateral-force derivative $C_{Y_\beta}$ shows little or no change among configurations or with increase in Mach number, all values being approximately -0.008.

4. The apparent aileron effectiveness parameter $\frac{pb}{2V}\Big/\delta_{a_t}$ shows a slight decrease with increase in wing span and area at supersonic speeds. The value of $\frac{pb}{2V}\Big/\delta_{a_t}$ remains nearly constant at 0.0026 up to a Mach number of about 0.90. With further increase in Mach number there is a gradual decrease in effectiveness to about 70 percent of the subsonic value at a Mach number of about 1.3.

5. Values of the control effectiveness derivatives $C_{l_{\delta_{a_t}}}$, $C_{n_{\delta_{a_t}}}$, $C_{l_{\delta_r}}$, and $C_{n_{\delta_r}}$ show little change among the configurations. The aileron effectiveness derivative $C_{l_{\delta_{a_t}}}$ decreases rather rapidly from an essentially constant value of about 0.0009 to 0.0010 in the transonic range to less than one-half that value at a Mach number of 1.25. A similar trend is evident in the rudder effectiveness derivative $C_{n_{\delta_r}}$ with subsonic values near -0.0005 to -0.0006 and supersonic values approaching -0.0001 at a Mach number of approximately 1.35. The yawing moment due to aileron deflection $C_{n_{\delta_{a_t}}}$ shows little change with change of Mach number, the values being about 0.0002. The rolling moment due to rudder deflection $C_{l_{\delta_r}}$ is essentially constant at about 0.0001 below a Mach number of 1.0. At the highest Mach numbers of the tests $C_{l_{\delta_r}}$ decreases to zero, however.


High-Speed Flight Station,
    National Advisory Committee for Aeronautics,
        Edwards, Calif., December 20, 1956.

APPENDIX


Lateral Equations of Motion

In determination of the control derivatives $C_{n_{\delta_r}}$, $C_{n_{\delta_{a_t}}}$, $C_{l_{\delta_{a_t}}}$, and $C_{l_{\delta_r}}$ from rudder pulses and abrupt aileron rolls the following procedure was used:  The abrupt rudder or aileron input was performed from trim level-flight conditions and only the first few tenths of one second of the control input were analyzed.  During this time interval the airplane experiences angular acceleration but there is not sufficient time for appreciable angular velocities or displacements to take place. Therefore, taking the equations of motion of the airplane relative to the X- and Z-body axes

$$C_l qSb \approx \dot{p}I_X - \dot{r}I_{XZ} + \left(I_Z - I_Y\right)qr - pqI_{XZ}$$

$$C_n qSb \approx \dot{r}I_Z - \dot{p}I_{XZ} + \left(I_Y - I_X\right)pq + qrI_{XZ}$$


Then, disregarding the terms with the product of angular velocities because of their minute values, the equations are transformed to

$$C_l = \frac{I_X\dot{p} - I_{XZ}\dot{r}}{qSb}$$

$$C_n = \frac{I_Z\dot{r} - I_{XZ}\dot{p}}{qSb}$$


The angular accelerations, velocities, and control deflections were obtained and the rolling-moment and yawing-moment coefficients were calculated and plotted against the control deflections.  From the plots of $C_n$ against $\delta_r$, $C_n$ against $\delta_{a_t}$, $C_l$ against $\delta_{a_t}$, and $C_l$ against $\delta_r$ the slopes (control derivatives) were obtained.

Again, it should be noted that all derivatives used in this paper are based on the physical dimensions of the particular configuration under consideration.

REFERENCES

1. Drake, Hubert M., Finch, Thomas W., and Peele, James R.:  Flight
   Measurements of Directional Stability to a Mach Number of 1.48 for
   an Airplane Tested With Three Different Vertical Tail Configurations.
   NACA RM H55G26, 1955.

2. Wolowicz, Chester H.:  Time-Vector Determined Lateral Derivatives of
   a Swept-Wing Fighter-Type Airplane With Three Different Vertical
   Tails at Mach Numbers Between 0.70 and 1.48.  NACA RM H56C20, 1956.

3. NACA High-Speed Flight Station:  Flight Experience With Two High-Speed
   Airplanes Having Violent Lateral-Longitudinal Coupling in Aileron
   Rolls.  NACA RM H55A13, 1955.

4. Finch, Thomas W., Peele, James R., and Day, Richard E.:  Flight
   Investigation of the Effect of Vertical-Tail Size on the Rolling
   Behavior of a Swept-Wing Airplane Having Lateral-Longitudinal
   Coupling.  NACA RM H55L28a, 1956.

5. Sisk, Thomas R., Andrews, William H., and Darville, Robert W.:  Flight
   Evaluation of the Lateral Stability and Control Characteristics of
   the Convair YF-102 Airplane.  NACA RM H56G11, 1956.

TABLE I

PHYSICAL CHARACTERISTICS OF AIRPLANE

| | Basic wing | Basic wing plus wing-tip extensions |
|---|---|---|
| **Wing:** | | |
| Airfoil section . . . . . . . . . . . . . . . . . . . . . . . . . . . . NACA | 64A007 | NACA 64A007 |
| Total area (including aileron and 83.84 sq ft covered by fuselage), sq ft . . . . . . . | 376.02 | 385.21 |
| Span, ft . . . . . . . . . . . . . . . . . . . . . . . . . . . . . . . . . . . . . | 36.58 | 38.58 |
| Mean aerodynamic chord, ft . . . . . . . . . . . . . . . . . . . . . . . . . . . | 11.33 | 11.16 |
| Root chord, ft . . . . . . . . . . . . . . . . . . . . . . . . . . . . . . . . . | 15.86 | 15.86 |
| Tip chord, ft . . . . . . . . . . . . . . . . . . . . . . . . . . . . . . . . . . | 4.76 | 4.15 |
| Taper ratio . . . . . . . . . . . . . . . . . . . . . . . . . . . . . . . . . . . | 0.30 | 0.262 |
| Aspect ratio . . . . . . . . . . . . . . . . . . . . . . . . . . . . . . . . . . | 3.56 | 3.86 |
| Sweep at 0.25 chord line, deg . . . . . . . . . . . . . . . . . . . . . . . . . . | 45 | 45 |
| Incidence, deg . . . . . . . . . . . . . . . . . . . . . . . . . . . . . . . . . | 0 | 0 |
| Dihedral, deg . . . . . . . . . . . . . . . . . . . . . . . . . . . . . . . . . . | 0 | 0 |
| Geometric twist, deg . . . . . . . . . . . . . . . . . . . . . . . . . . . . . . | 0 | 0 |
| **Aileron:** | | |
| Area rearward of hinge line (each), sq ft . . . . . . . . . . . . . . . . . . . | 19.32 | 19.32 |
| Span at hinge line (each), ft . . . . . . . . . . . . . . . . . . . . . . . . . | 7.81 | 7.81 |
| Chord rearward of hinge line, percent wing chord . . . . . . . . . . . . . . . . | 25 | 25 |
| Travel (each), deg . . . . . . . . . . . . . . . . . . . . . . . . . . . . . . . | ±15 | ±15 |
| **Leading-edge slat:** | | |
| Span, equivalent, ft . . . . . . . . . . . . . . . . . . . . . . . . . . . . . . | 12.71 | 12.71 |
| Segments . . . . . . . . . . . . . . . . . . . . . . . . . . . . . . . . . . . . | 5 | 5 |
| Spanwise location, inboard end, percent wing semispan . . . . . . . . . . . . . | 24.6 | 23.3 |
| Spanwise location, outboard end, percent wing semispan . . . . . . . . . . . . . | 94.1 | 89.2 |
| Ratio of slat chord to wing chord (parallel to fuselage reference line), percent . . . | 20 | 20 |
| Rotation, maximum, deg . . . . . . . . . . . . . . . . . . . . . . . . . . . . . | 15 | 15 |

| | |
|---|---|
| **Horizontal tail:** | |
| Airfoil section . . . . . . . . . . . . . . . . . . . . . . . . . . . . . . . . . . . . NACA | 65A003.5 |
| Total area (including 31.65 sq ft covered by fuselage), sq ft . . . . . . . . . . . . . . . | 98.86 |
| Span, ft . . . . . . . . . . . . . . . . . . . . . . . . . . . . . . . . . . . . . . . . | 18.72 |
| Mean aerodynamic chord, ft . . . . . . . . . . . . . . . . . . . . . . . . . . . . . . | 5.83 |
| Root chord, ft . . . . . . . . . . . . . . . . . . . . . . . . . . . . . . . . . . . . . | 8.14 |
| Tip chord, ft . . . . . . . . . . . . . . . . . . . . . . . . . . . . . . . . . . . . . . | 2.46 |
| Taper ratio . . . . . . . . . . . . . . . . . . . . . . . . . . . . . . . . . . . . . . | 0.30 |
| Aspect ratio . . . . . . . . . . . . . . . . . . . . . . . . . . . . . . . . . . . . . . | 3.54 |
| Sweep at 0.25 chord line, deg . . . . . . . . . . . . . . . . . . . . . . . . . . . . . | 45 |
| Dihedral, deg . . . . . . . . . . . . . . . . . . . . . . . . . . . . . . . . . . . . . | 0 |
| Travel, leading edge up, deg . . . . . . . . . . . . . . . . . . . . . . . . . . . . . . | 5 |
| Travel, leading edge down, deg . . . . . . . . . . . . . . . . . . . . . . . . . . . . . | 25 |
| Irreversible hydraulic boost and artificial feel | |

| | A | B | C |
|---|---|---|---|
| **Vertical tail:** | | | |
| Airfoil section . . . . . . . . . . . . . . . . . . . . . . | NACA 65A003.5 | NACA 65A003.5 | NACA 65A003.5 |
| Area (excluding dorsal fin and area blanketed by fuselage), sq ft . . . . . . . . . . . . . . . . . | 33.5 | 37.3 | 42.7 |
| Area blanketed by fuselage (area between fuselage contour line and line parallel to fuselage reference line through intersections of leading edge of vertical tail and fuselage contour line) . . . . . . . . . . . | 2.11 | 2.11 | 2.45 |
| Span (unblanketed), ft . . . . . . . . . . . . . . . . . . | 6.14 | 7.45 | 7.93 |
| Mean aerodynamic chord, ft . . . . . . . . . . . . . . | 5.83 | 5.51 | 5.90 |
| Root chord, ft . . . . . . . . . . . . . . . . . . . . . . | 7.75 | 7.75 | 8.28 |
| Tip chord, ft . . . . . . . . . . . . . . . . . . . . . . . | 3.32 | 2.32 | 2.49 |
| Taper ratio . . . . . . . . . . . . . . . . . . . . . . . . | 0.428 | 0.301 | 0.301 |
| Aspect ratio . . . . . . . . . . . . . . . . . . . . . . . | 1.13 | 1.49 | 1.49 |
| Sweep at 0.25 chord line, deg . . . . . . . . . . . . . | 45 | 45 | 45 |
| **Rudder:** | | | |
| Area, rearward of hinge line, sq ft . . . . . . . . . . . . | 6.3 | 6.3 | 6.3 |
| Span at hinge line, ft . . . . . . . . . . . . . . . . . . | 3.33 | 3.33 | 3.33 |
| Root chord, ft . . . . . . . . . . . . . . . . . . . . . . | 2.27 | 2.27 | 2.27 |
| Tip chord, ft . . . . . . . . . . . . . . . . . . . . . . . | 1.50 | 1.50 | 1.50 |
| Travel, deg . . . . . . . . . . . . . . . . . . . . . . . . | ±20 | ±20 | ±20 |
| Spanwise location, inboard end, percent vertical-tail span . . . . . . . . . . . . . . . | 4.5 | 3.7 | 3.1 |
| Spanwise location, outboard end, percent vertical-tail span . . . . . . . . . . . . . . | 58.2 | 48.0 | 44.8 |
| Chord, percent vertical-tail chord . . . . . . . . . . . | 30.0 | 30.0 | 28.4 |
| Aerodynamic balance . . . . . . . . . . . . . . . . . . | Overhanging, unsealed | Overhanging, unsealed | Overhanging, unsealed |

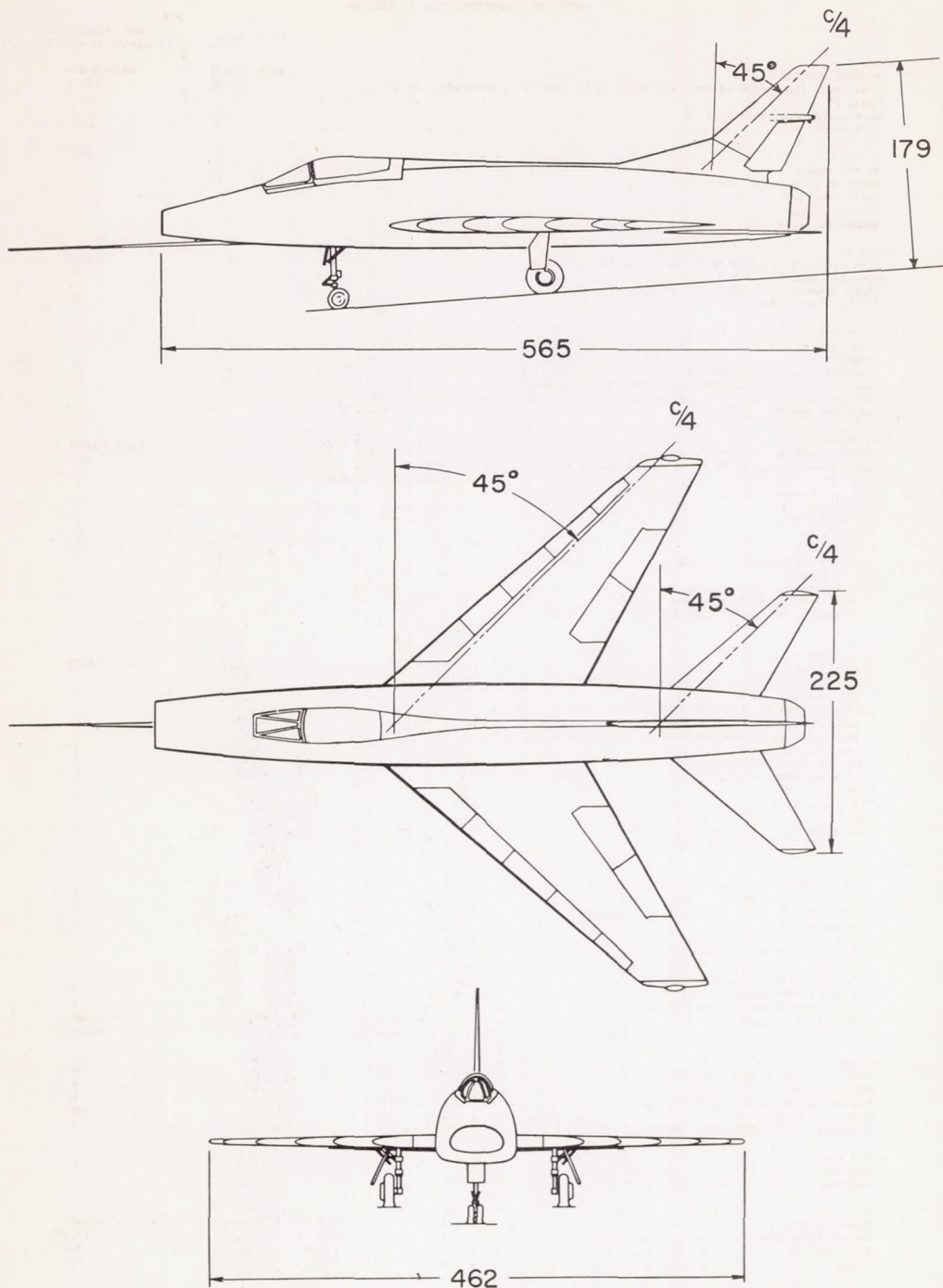| | |
|---|---|
| **Fuselage:** | |
| Length (afterburner nozzle closed), ft . . . . . . . . . . . . . . . . . . . . . . . . . . . . . . . . . . . . . . . | 45.64 |
| Maximum width, ft . . . . . . . . . . . . . . . . . . . . . . . . . . . . . . . . . . . . . . . . . . . . . . . . | 5.58 |
| Maximum depth over canopy, ft . . . . . . . . . . . . . . . . . . . . . . . . . . . . . . . . . . . . . . . . . . | 6.37 |
| Side area (total), sq ft . . . . . . . . . . . . . . . . . . . . . . . . . . . . . . . . . . . . . . . . . . . . . | 230.92 |
| Fineness ratio (afterburner nozzle closed) . . . . . . . . . . . . . . . . . . . . . . . . . . . . . . . . . . . . | 7.86 |
| **Speed brake:** | |
| Surface area, sq ft . . . . . . . . . . . . . . . . . . . . . . . . . . . . . . . . . . . . . . . . . . . . . . . | 14.14 |
| Maximum deflection, deg . . . . . . . . . . . . . . . . . . . . . . . . . . . . . . . . . . . . . . . . . . . . . | 50 |
| **Power plant:** | |
| Turbojet engine . . . . . . . . . . . . . . . . . . . . . . . . . . . . . . One Pratt & Whitney J57-P-7 with afterburner | |
| Thrust (guarantee sea level), afterburner, lb . . . . . . . . . . . . . . . . . . . . . . . . . . . . . . . . . . . | 15,000 |
| Military, lb . . . . . . . . . . . . . . . . . . . . . . . . . . . . . . . . . . . . . . . . . . . . . . . . . . . | 9,220 |
| Normal, lb . . . . . . . . . . . . . . . . . . . . . . . . . . . . . . . . . . . . . . . . . . . . . . . . . . . | 8,000 |
| **Airplane weight, lb:** | |
| Basic (without fuel, oil, water, pilot) . . . . . . . . . . . . . . . . . . . . . . . . . . . . . . . . . . . . . . | 19,662 |
| Total (full fuel, oil, water, pilot) . . . . . . . . . . . . . . . . . . . . . . . . . . . . . . . . . . . . . . . | 24,800 |
| **Center-of-gravity location, percent mean aerodynamic chord:** | |
| Total weight - gear down . . . . . . . . . . . . . . . . . . . . . . . . . . . . . . . . . . . . . . . . . . . . . | 31.80 |
| Total weight - gear up . . . . . . . . . . . . . . . . . . . . . . . . . . . . . . . . . . . . . . . . . . . . . . | 31.80 |

Figure 1.- Three-view drawing of the test airplane with the largest
    vertical tail and enlarged wing configuration.  All dimensions in
    inches.
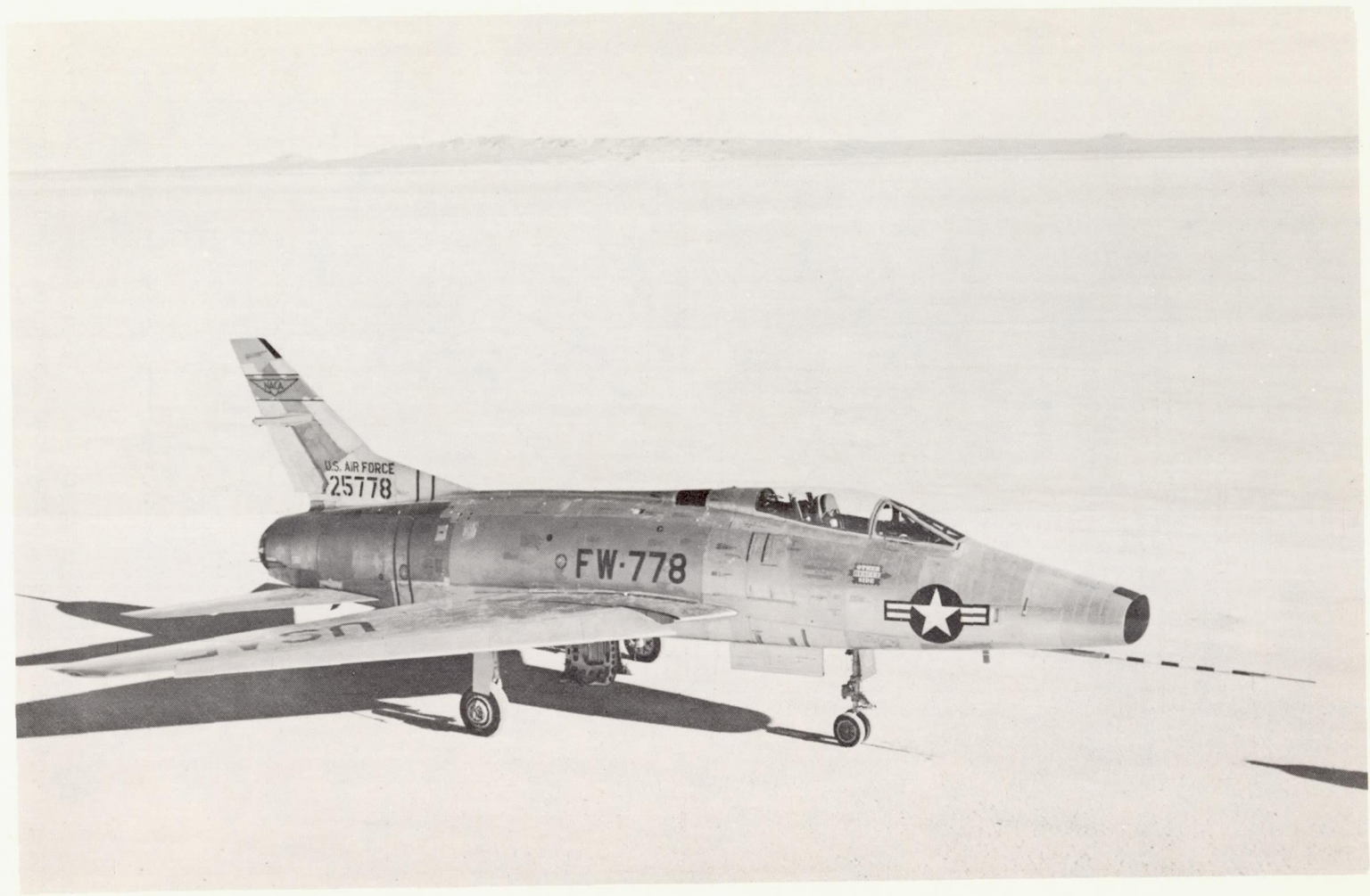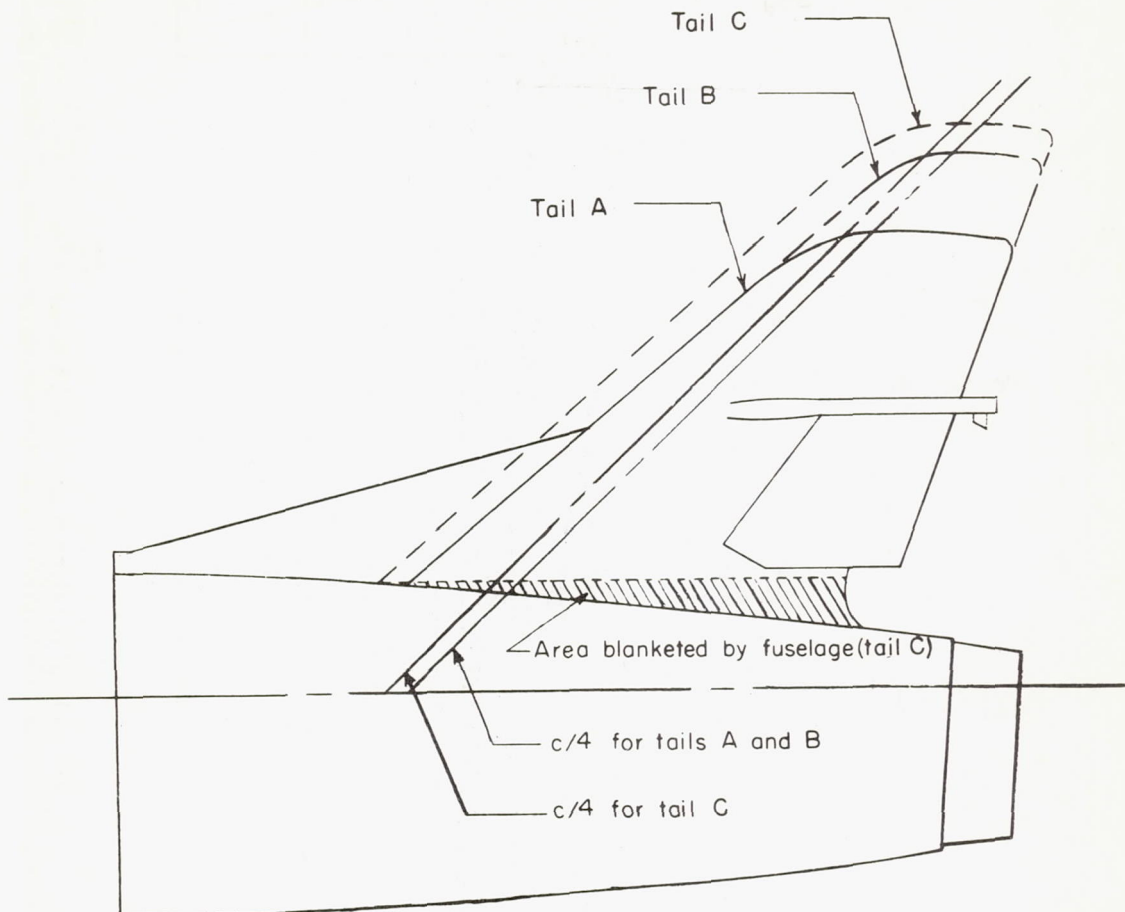
E-2097

Figure 2.- Photograph of the airplane with largest vertical-tail and enlarged-wing configuration.
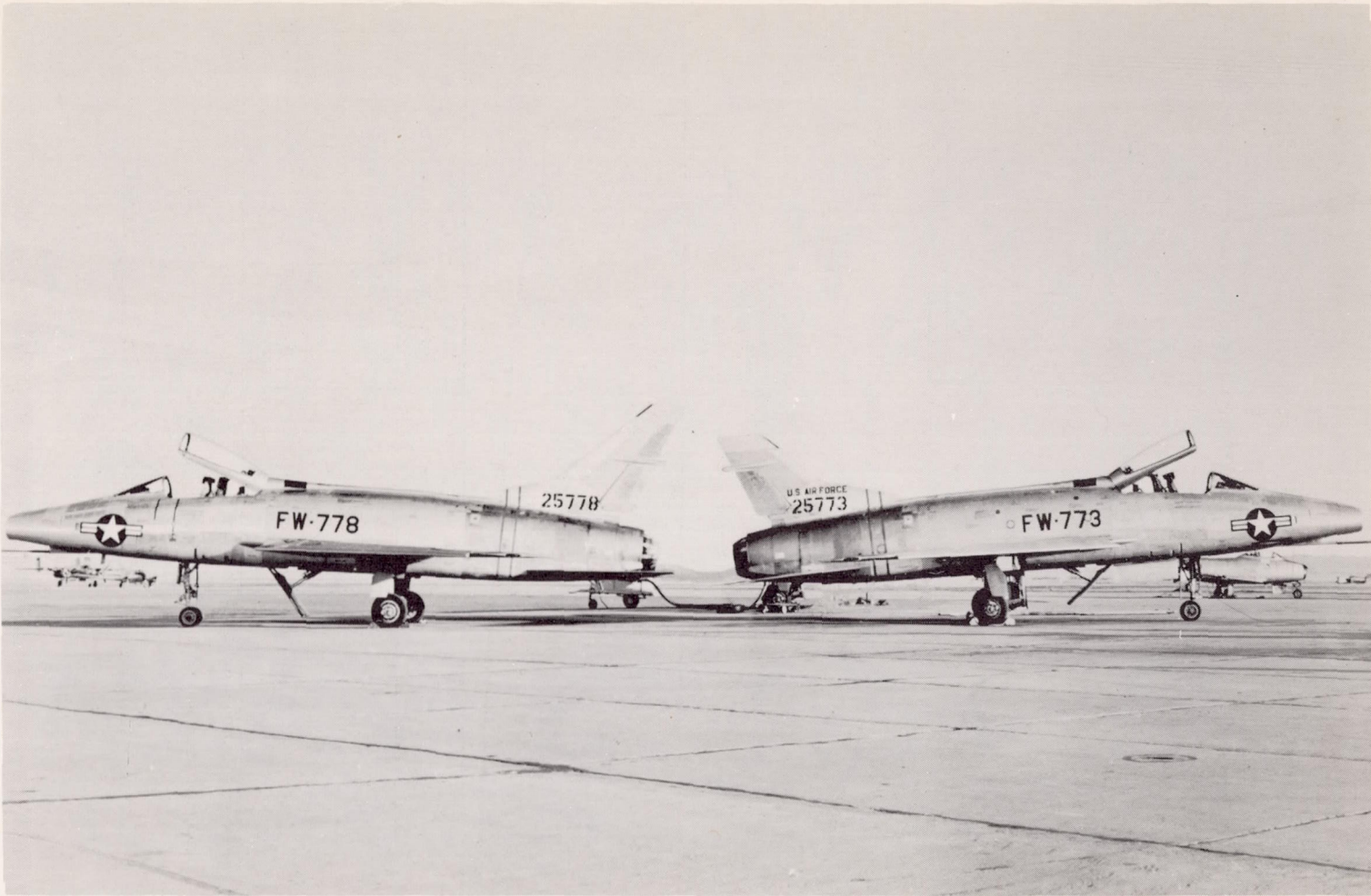
E-1622

Figure 3.- Photograph of two airplanes showing tails A and C.

| Tail | $\Lambda_{c/4}$, deg | A | $\lambda$ | Area, sq ft (1) | Span, ft (2) | Blanketed area, sq ft |
|------|------|------|------|------|------|------|
| A | 45° | 1.13 | 0.428 | 33.5 | 6.14 | 2.11 |
| B | 45° | 1.49 | 0.301 | 37.3 | 7.45 | 2.11 |
| C | 45° | 1.49 | 0.301 | 42.7 | 7.93 | 2.45 |

(1)  Area not blanketed by fuselage

(2)  Span not blanketed by fuselage

Figure 4.- Sketch of vertical tails A, B, and C.
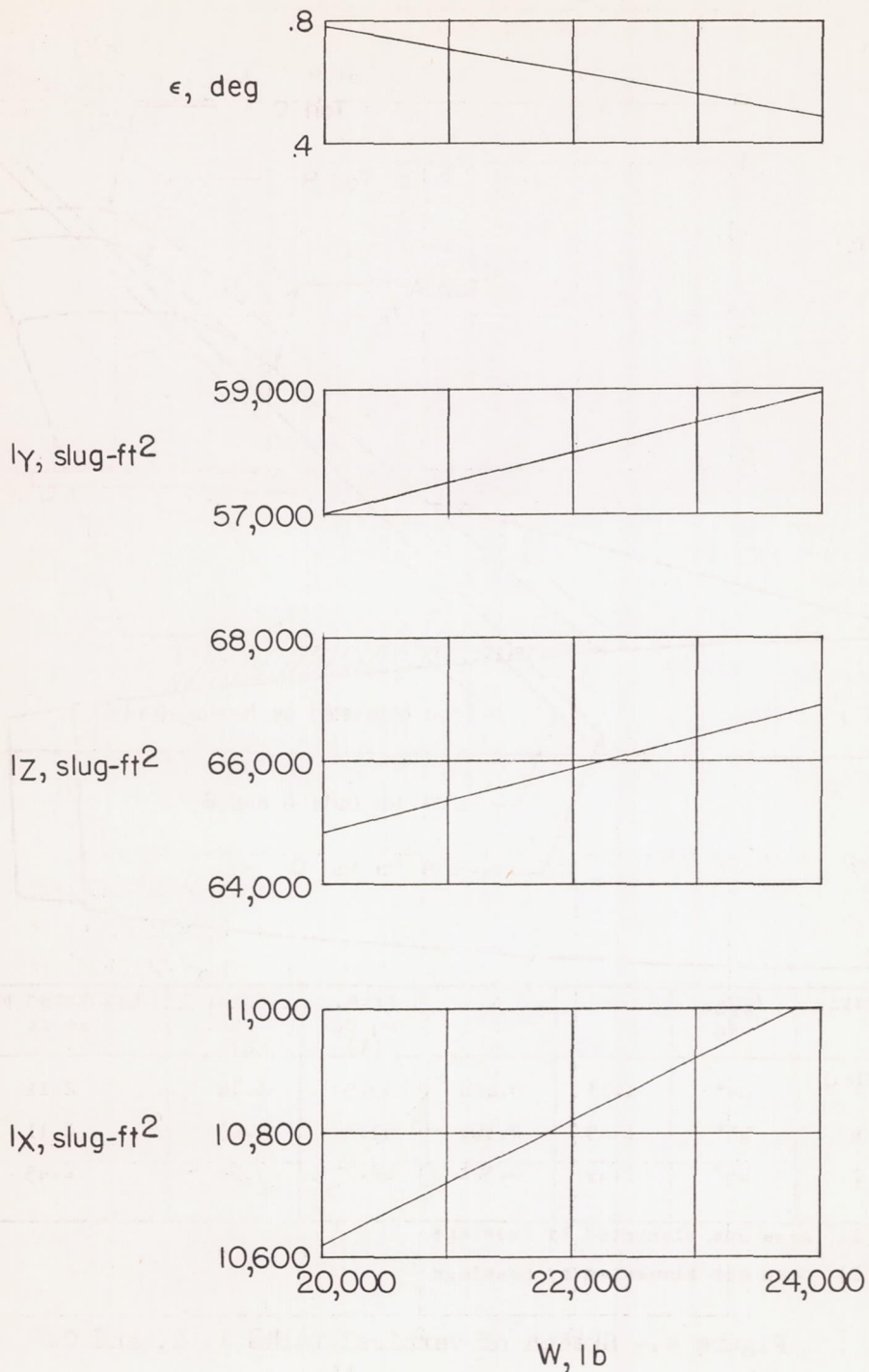
Figure 5.- Approximated variation of the principal moments of inertia and inclination of principal axis relation to the body axis.
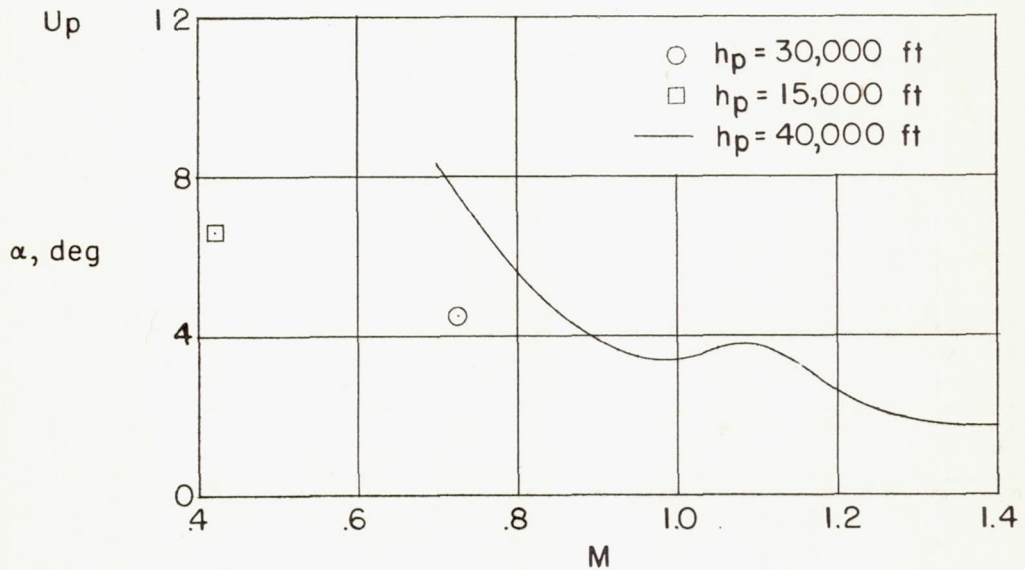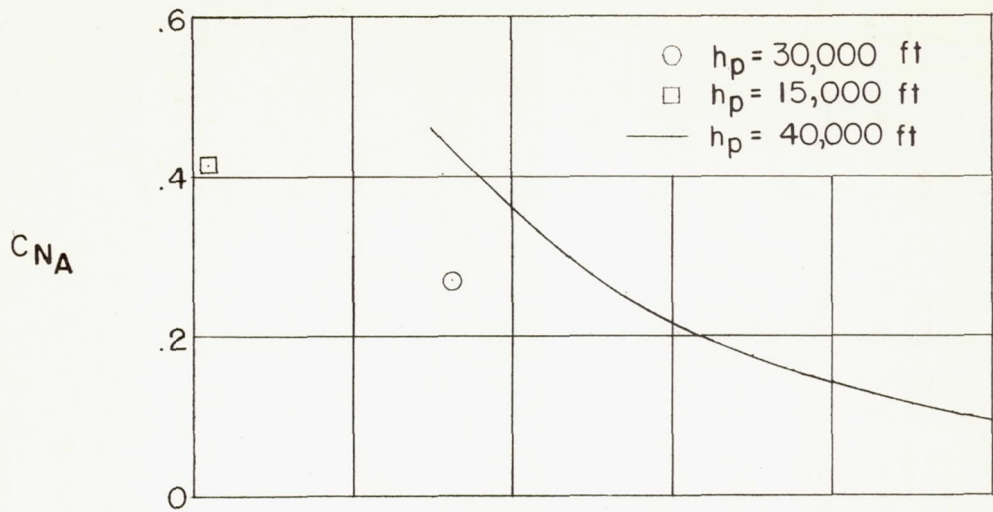
Figure 6.- Variation of trim normal-force coefficient and angle of attack with Mach number for 1 g flight, and a nominal weight of 22,000 pounds.
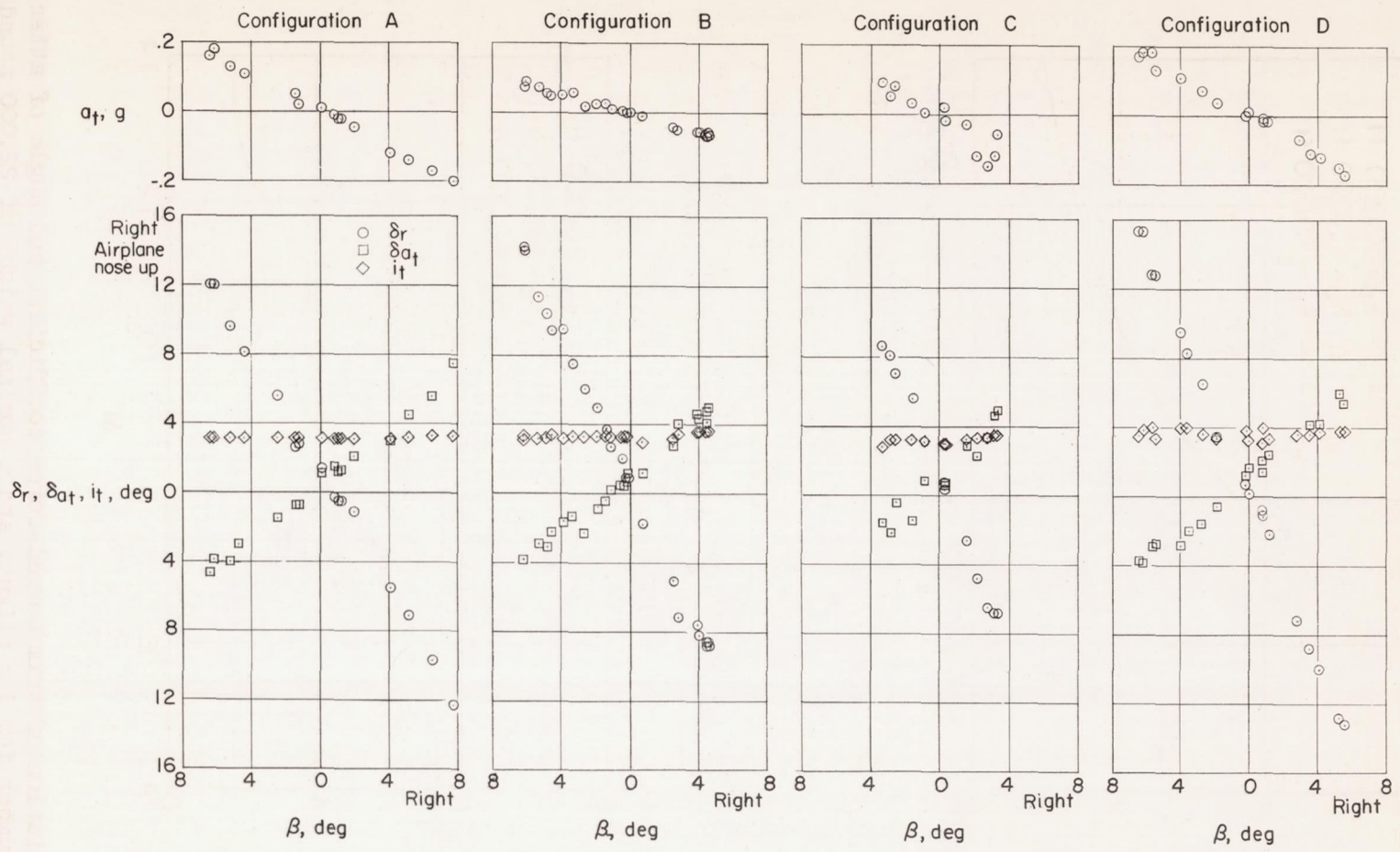
(a)  M = 0.735; $h_p$ = 30,000 feet.

Figure 7.- Characteristics in sideslip.
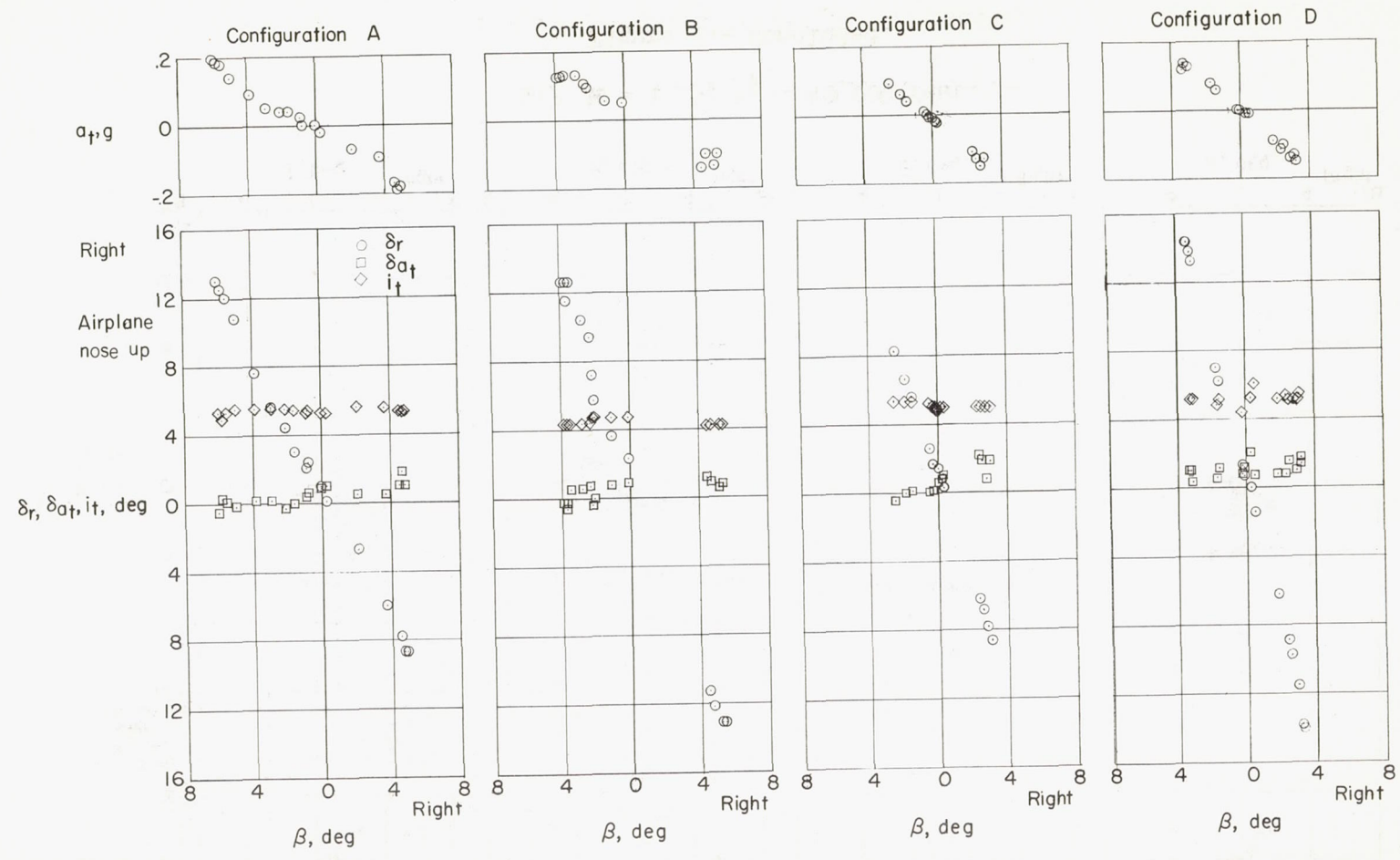
(b)  M = 1.00; h_p = 40,000 feet.

Figure 7.- Continued.
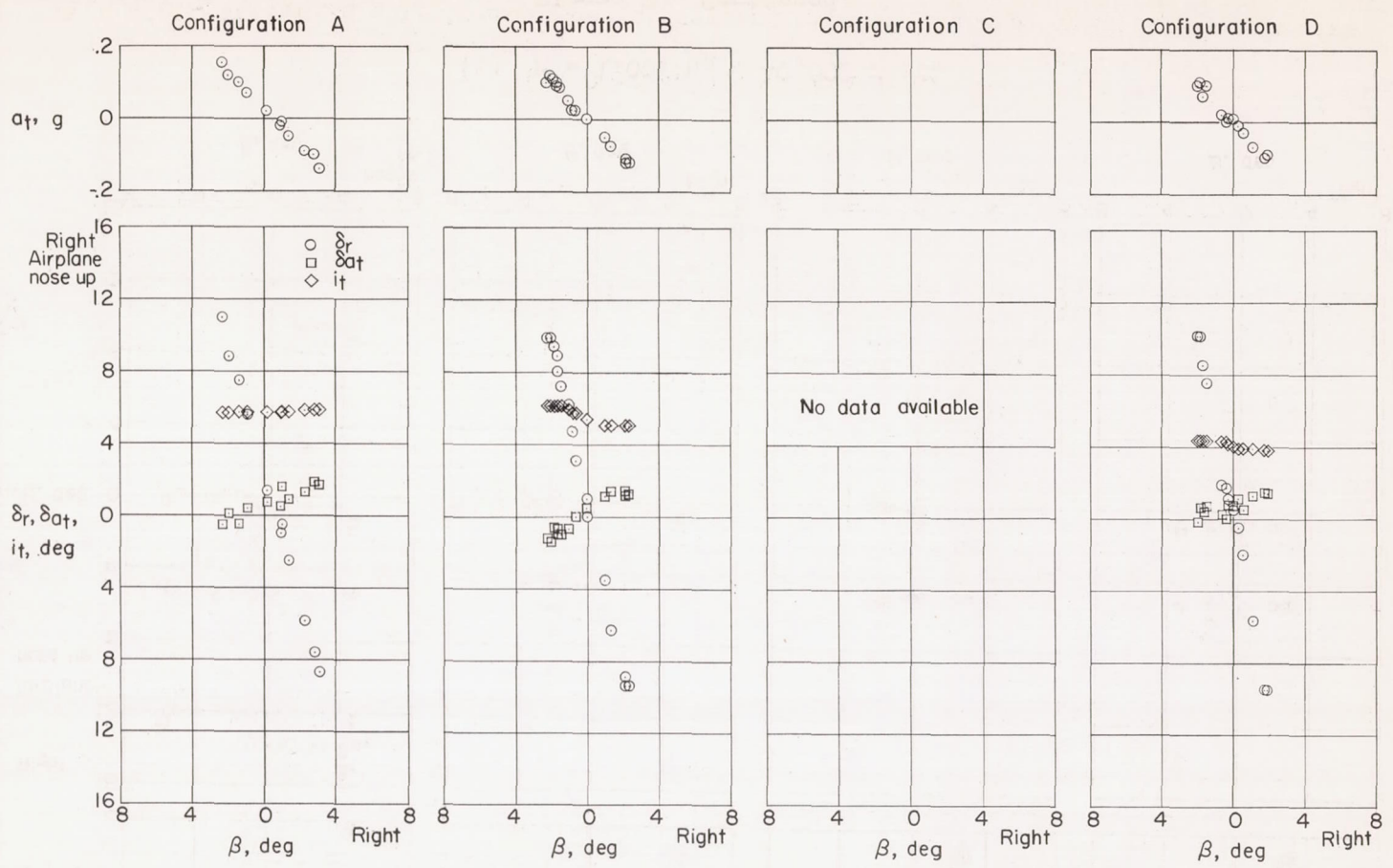
(c)  M = 1.15; $h_p$ = 40,000 feet.

Figure 7.- Concluded.
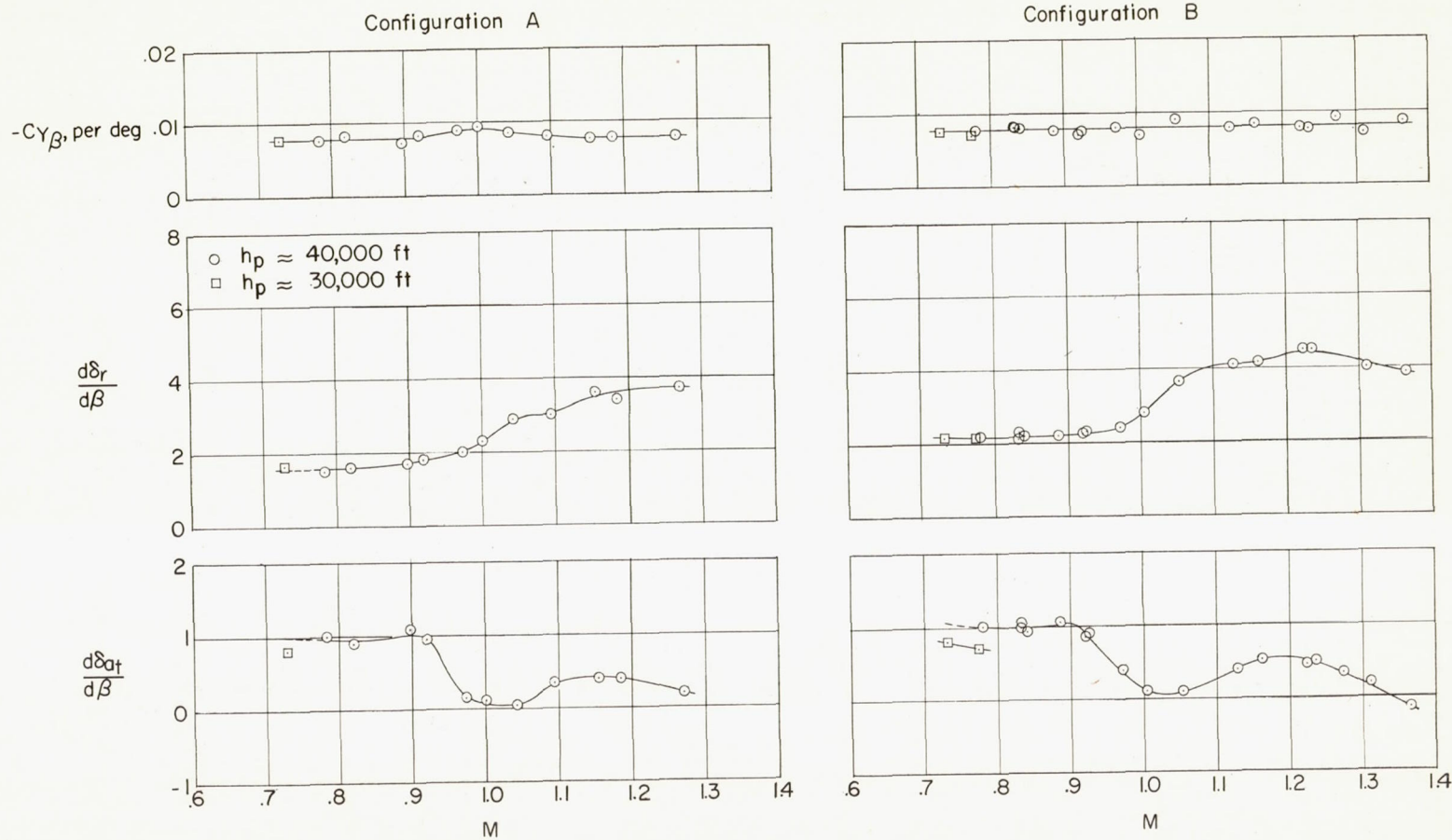
(a) Configurations A and B.

Figure 8.- Variation with Mach number of several apparent lateral stability parameters.

Configuration C
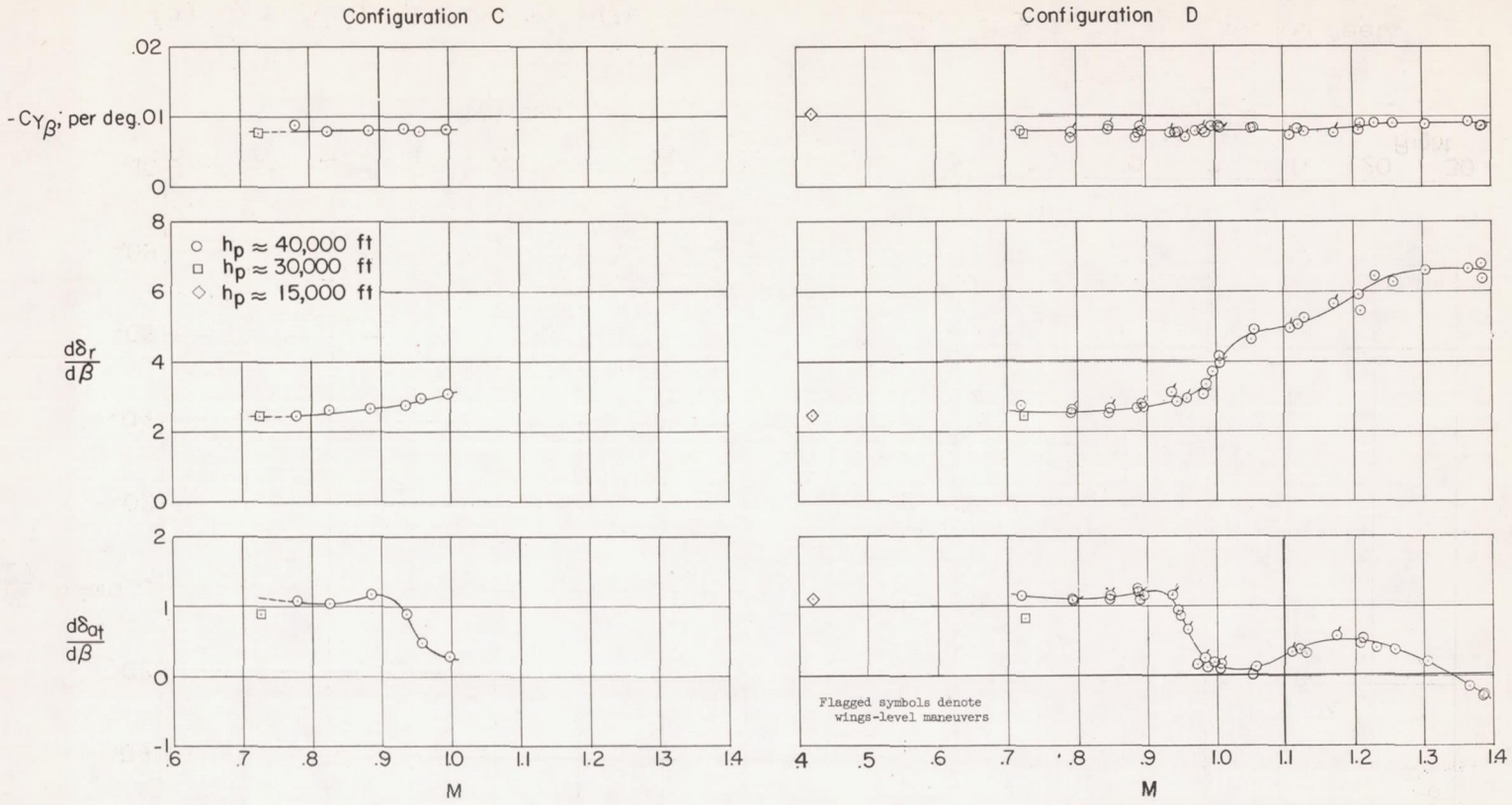
Configuration D



(b) Configurations C and D.

Figure 8.- Concluded.
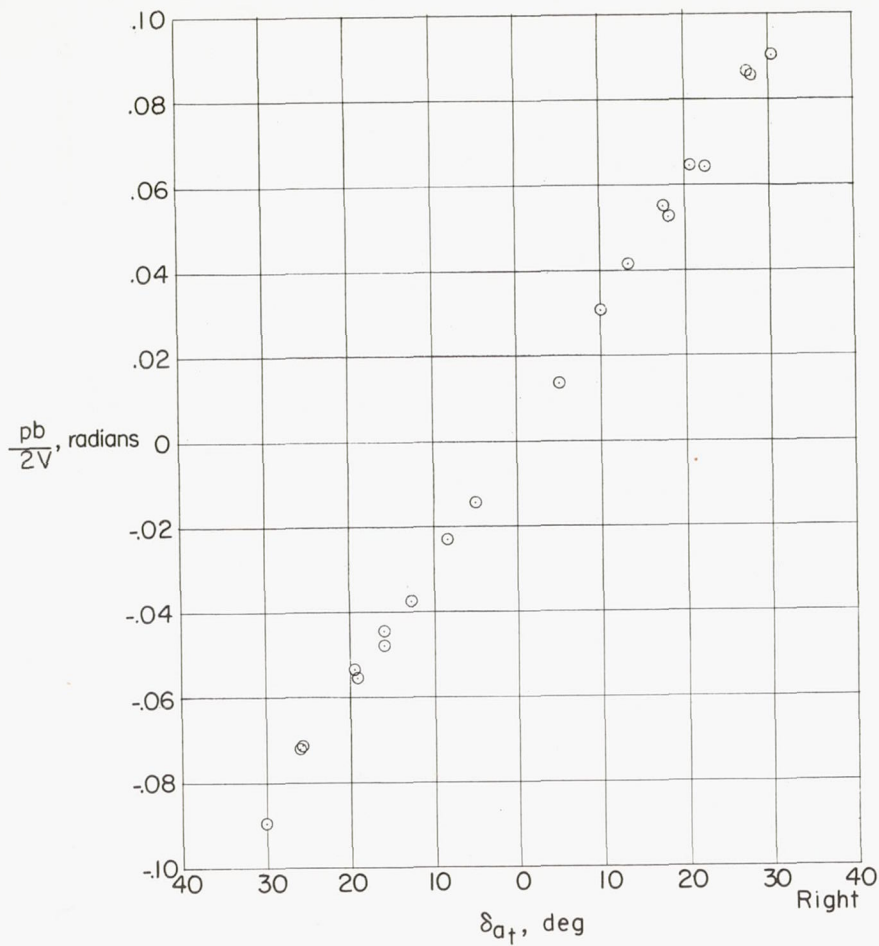
(a)  M = 0.73; $h_p$ = 30,000 feet.
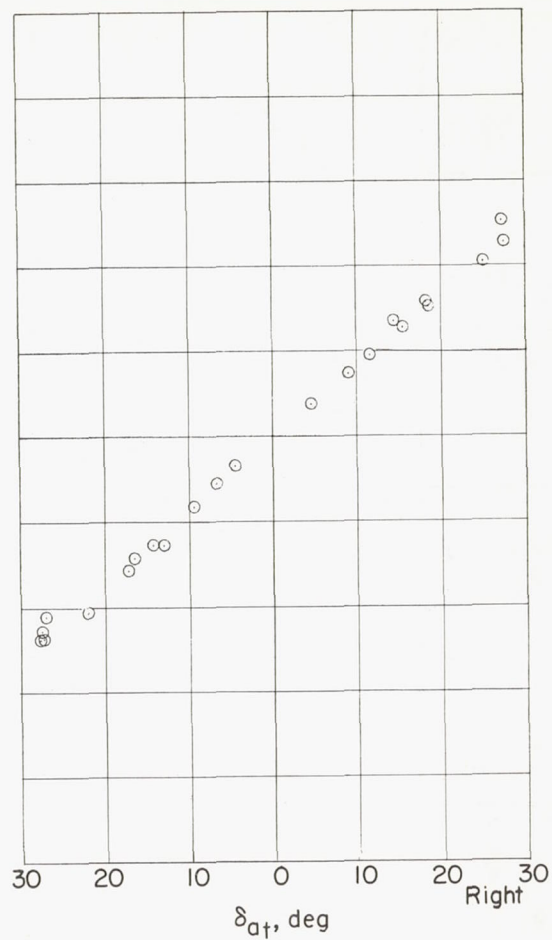
(b)  M = 1.25; $h_p$ = 40,000 feet.

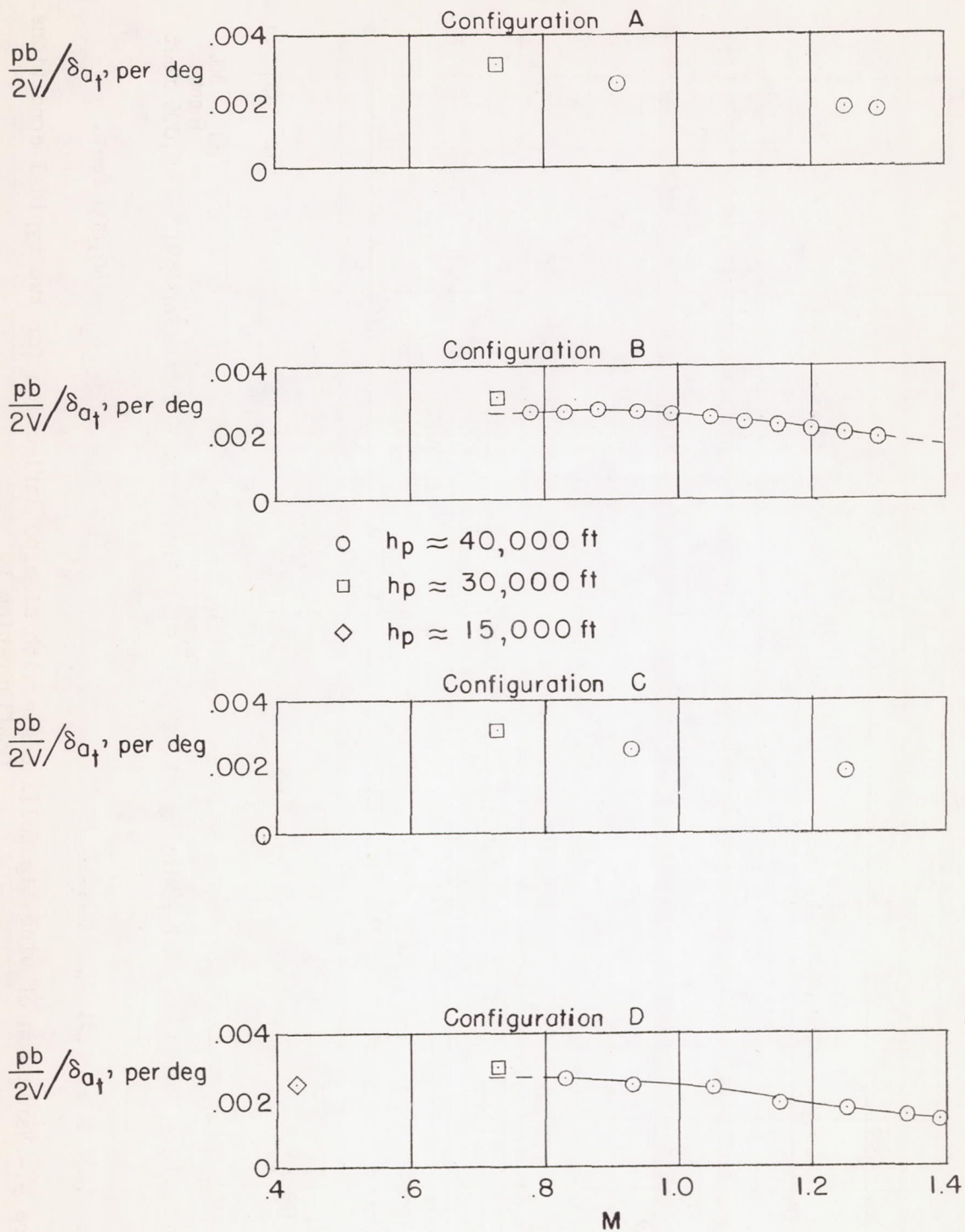Figure 9.- Variation of wing-tip helix angle with aileron deflection for two typical conditions. Configuration D.

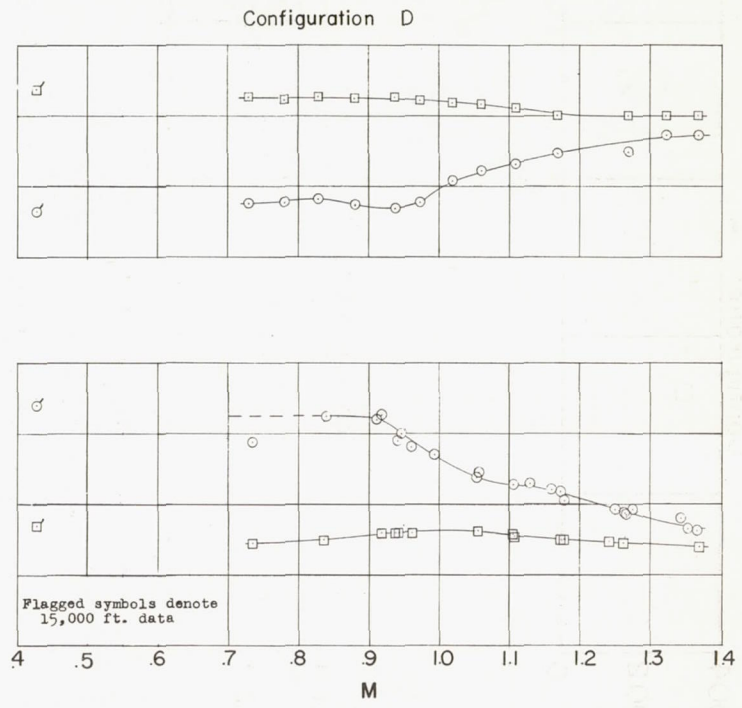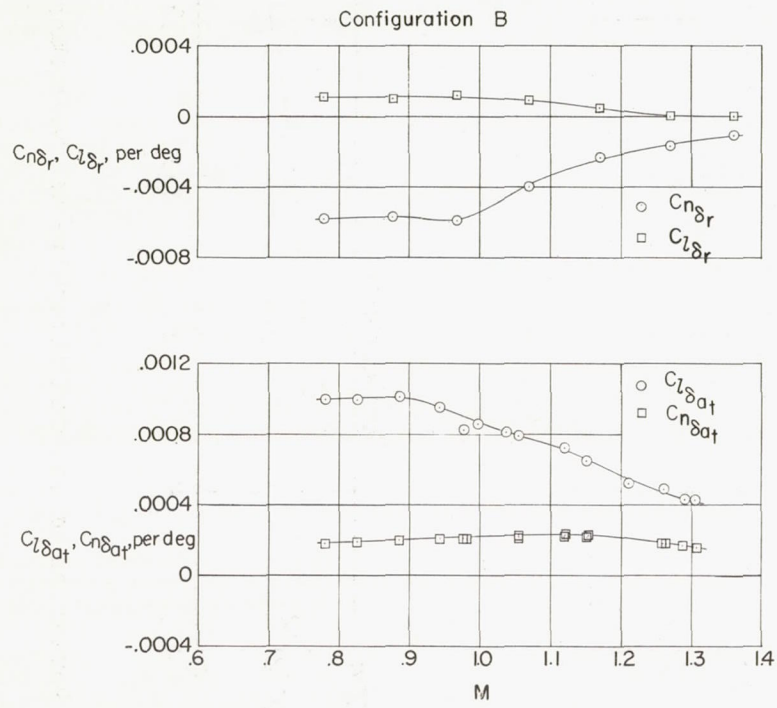Figure 10.- Variation of aileron effectiveness with Mach number.

Figure 11.- Variation with Mach number of control effectiveness parameters; $h_p$ = 40,000 feet with exceptions noted.